Oncogene (2004) 00, 1–9
© 2004 Nature Publishing Group All rights reserved 0950-9232/04 $25.00
www.nature.com/onc

ORIGINAL PAPER

Carcinogen-induced colon tumors in mice are chromosomally stable and are characterized by low-level microsatellite instability

Kishore Guda[1,3], Madhvi B Upender[2,3], Glenn Belinsky[1], Christopher Flynn[1], Masako Nakanishi[1], Jillian N Marino[1], Thomas Ried*[,2] and Daniel W Rosenberg[1]

[1]*Center for Molecular Medicine, University of Connecticut Health Center, Farmington, CT 06030-3101, USA;* [2]*Genetics Branch, Center for Cancer Research, National Cancer Institute/NIH, 50 South Drive, Room 1306, Bethesda, MD 20892-8010, USA*

The azoxymethane (AOM)-induced mouse colon tumor model recapitulates many of the histopathological features associated with the multistage progression of human sporadic colorectal cancers (CRCs). To better define the genetic events associated with tumorigenesis in this murine model, we analysed tumors from A/J mice for chromosomal (CIN) and microsatellite (MSI) instabilities, two fundamental pathways of genomic instability that play a critical role in the pathogenesis of human CRCs. Male A/J mice, 6-week old, were injected with either AOM ($n=5$) (10 mg/kg b.w., i.p.) or vehicle ($n=5$) (0.9% NaCl solution) once a week for 6 weeks. At 32 weeks after the last dose, comparative genomic hybridization (CGH) was performed on 16 tumors harvested from five animals. Although 25% of the tumors displayed either a gain of chromosome 2 or loss of Y, the majority (75%) showed no genomic imbalances. Further analysis of chromosomal aberrations, using CGH and spectral karyotyping (SKY) techniques, was performed in our recently established A/J colon tumor-derived cell line, AJ02-NM0. Results showed a pseudotetraploid karyotype with loss of only the Y chromosome in these cultured cells, thereby providing additional evidence for the minimal role of CIN in the primary AOM-induced tumors. Interestingly, the majority (81%) of A/J tumors displayed low-level microsatellite instability (MSI-L) when analysed using mono- and dinucleotide repeat markers, and showed a significant expansion to high-level instability (MSI-H) in the AJ02-NM_0 cells. This finding in cultured cells additionally provides evidence that a mild mutator pathway may contribute to the development of behaviorally benign carcinomas *in situ* in A/J mice. To better understand the tumorigenic process in the A/J colons, we screened for mutational alterations in key regions of the K-*ras* and *Apc* genes. Results showed a very low frequency (6%) of K-*ras* activating mutations, together with the absence of *Apc* truncation mutations in primary tumors and AJ02-NM_0 cells. However, these tumors displayed intense nuclear accumulation of β-catenin protein, indicating activation of the Wnt signaling pathway. Based on our molecular and cytogenetic findings, we propose that carcinogen-induced tumors may develop via mechanisms independent of the 'classical' CIN or MSI pathways.

Oncogene (2004) **0,** 000–000. doi:10.1038/sj.onc.1207489

Keywords: azoxymethane; mice; colon tumorigenesis; chromosomal instability; spectral karyotyping; microsatellite instability

Introduction

Colorectal cancer (CRC) is the second leading cause of cancer deaths in the US. Although significant molecular insights have been gained by a direct analysis of human CRCs, animal models provide an important experimental tool for elucidating the early molecular alterations that underlie the pathogenesis of both familial and nonfamilial (sporadic) forms of the disease (Corpet and Pierre, 2003). In particular, the azoxymethane (AOM)-tumor model has been used extensively to identify molecular mechanisms involved in the multistage progression of sporadic CRCs (Corpet and Pierre, 2003). In mice, repetitive administration of this methylating carcinogen produces noninvasive *in situ* adenocarcinomas, specifically within the distal colons of susceptible strains (Nambiar *et al*., 2003). More importantly, AOM-induced tumors in mice exhibit pathological and molecular features that recapitulate those seen in sporadic forms of the human disease (Wang *et al*., 1998; Guda *et al*., 2001; Nambiar *et al*., 2002; Dong *et al*., 2003).

There is increasing evidence that genomic instability plays an important role in the progression of human colorectal tumors (Lindblom, 2001; Hoglund *et al*., 2002; Goel *et al*., 2003). Two independent pathways of genomic instability have been identified; chromosomal (CIN) and microsatellite (MSI) instability (Fearon and Vogelstein, 1990; Lengauer *et al*., 1997). CIN or the 'suppressor' pathway is the predominant form of genetic instability, manifested by widespread cytogenetic abnormalities, including chromosomal gains, losses, and rearrangements (Rajagopalan *et al*., 2003). CIN and aneuploidy, however, are not random. In fact, chromo-

*Correspondence: T Ried; E-mail: riedt@mail.nih.gov
[3]These authors contributed equally to the work
Received 26 November 2003; revised 5 January 2003; accepted 6 January 2004

UNCORRECTED PROOF

Gml : Ver 6.0Ver 6.0
Journal: ONC Disk used Despatch Date: 28/1/2004
Article : NPG_ONC_7269r Pages: 1–9 OP: Raj Ed: Pouly Scan: Deepa

some banding analyses and comparative genomic hybridization (CGH) have firmly established that colorectal carcinomas are defined by a conserved distribution of chromosomal gains (7, 8q, 11q, 13q, and 20q) and losses (1p, 18q, 8p, and 17p) (Ried *et al*., 1996; Hermsen *et al*., 2002; Hoglund *et al*., 2002; Goel *et al*., 2003). On the other hand, MSI or the 'mutator' pathway is characterized by the progressive accumulation of somatic alterations in the length of simple, repeat nucleotide sequences known as microsatellites, and is a hallmark of tumors that develop within the colons of HNPCC patients. In addition, ~10–15% of sporadic colorectal carcinoma cases show evidence of high-level MSI (MSI-H). MSI-H CRCs do not exhibit gross cytogenetic abnormalities and, in general, have a diploid karyotype (Lothe *et al*., 1993; Thibodeau *et al*., 1993; Olschwang *et al*., 1997; Eshleman *et al*., 1998). While defects in the DNA mismatch repair system are attributable to an MSI phenotype, the precise molecular mechanisms leading to CIN remain to be elucidated (Young *et al*., 2001; Rajagopalan *et al*., 2003).

The following study was undertaken to gain further insight into the molecular mechanisms that underlie AOM-induced colon tumorigenesis. We have undertaken a comprehensive set of studies to assess the potential contributions of CIN and MSI in carcinogen-induced tumors in A/J mice, using a combined approach of CGH and microsatellite analyses. Our results suggest that carcinogen-induced tumors may develop via mechanisms independent of the 'classical' CIN or MSI pathways, and that the tumors that form in A/J mice are representative of human adenomas or carcinomas *in situ*.

Results

Histopatholgic examination of AOM-induced colon tumors

Hematoxylin and eosin-stained sections were examined microscopically to confirm the histologic characteristics of AOM-induced colon tumors in A/J mice. These tumors display the typical features of an *in situ* adenocarcinoma, including marked cellular atypia, loss of goblet cell differentiation, nuclear pseudostratification, and a high nucleus to cytoplasmic ratio (Figure 1) (Nambiar *et al*., 2003). However, we rarely observe breachment of the basement membrane within the tumor mass and never find evidence for metastatic tumor dissemination (Nambiar *et al*., 2003). The histopathological evidence showing lack of invasion by the tumor crypts in the present study (Figure 1) further highlights these previous observations.

CIN is infrequent in carcinogen-induced colon tumors

Given the fact that CIN and aneuploidy are typically nonrandom events associated with human CRCs (Ried *et al*., 1996, 1999; Hermsen *et al*., 2002; Hoglund *et al*., 2002; Goel *et al*., 2003; Rajagopalan *et al*., 2003), we determined whether a specific pattern of chromosomal imbalance(s) also occurs in AOM-induced tumors. As shown in Table 1, the majority (12/16) of AOM-induced tumors showed no gross chromosomal aberrations by CGH. The remaining four tumors displayed either a gain of chromosome 2 or loss of the Y chromosome (Table 1, Figure 2).

After completion of the CGH analysis in the primary tumors, we tested the extent of CIN in our recently

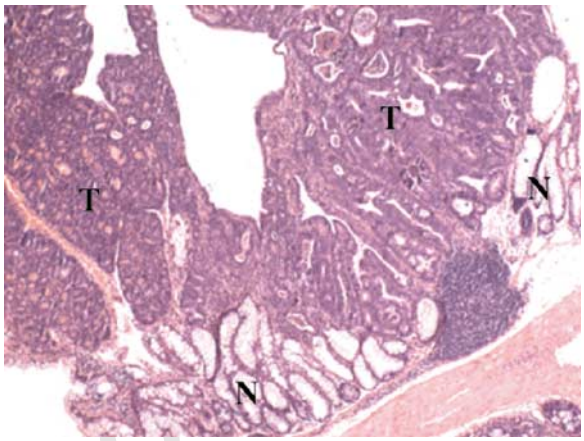

Figure 1 Histologic appearance of an AOM-induced colon tumor. Representative photomicrograph of a hematoxylin and eosin-stained *in situ* adenocarcinoma section from an A/J mouse. Note the exophytic appearance, marked cellular atypia, loss of goblet cell differentiation, nuclear pseudostratification, and a high nucleus-to-cytoplasmic ratio with no evidence for submucosal invasion. T, tumor tissue; N, adjacent normal-appearing crypts

Table 1 Summary of chromosomal and microsatellite instabilities in AOM-induced colon tumors in A/J mice

Tumors	*Chromosomal aberrations detected by CGH*	*Unstable microsatellite loci by MSI analysis*
A1	None	*D17Mit72, D15Mit93*
A2	None	*D17Mit72, D15Mit93*
A3	None	*D17Mit72, D15Mit93*
B1	None	*None*
B2	None	*None*
B3	None	*None*
C1	−Y	*D10Mit2, D15Mit93*
C2	−Y	*D10Mit2, D15Mit93*
C3	None	*D10Mit2, D15Mit93*
C4	None	*D10Mit2, D15Mit93*
D1	None	*D10Mit2, D15Mit93*
D2	None	*D10Mit2, D15Mit93*
D3	None	*D10Mit2, D15Mit93*
E1	+2	*D15Mit93*
E2	+2	*D15Mit93*
E3	None	*D15Mit93*
AJ02-NM0 cells	−4, −14, −Y	*uPAR, D10Mit2, D1Mit4, D14Mit15, D7Mit17, D1Mit62, D17Mit72, D15Mit93, D17Mit123*

The CGH and MSI profiles of A/J tumors and AJ02-NM_0 cells are shown in the table. DNA extracted from 16 tumors isolated from five individual mice (A–E), in addition to AJ02-NM_0 cells, was used for these analyses. The (−) and (+) signs indicate losses and gains of chromosomes, respectively

UNCORRECTED PROOF

established colon tumor cell line, AJ02-NM0. Results from CGH and SKY analyses of the AJ02-NM_0 cells also identified the loss of the Y chromosome, consistent with a subset of the primary tumors (Table 1, Figure 3). Furthermore, of the 20 metaphase spreads analysed by SKY, no structural chromosomal rearrangements were evident, and the number of chromosomes per cell ranged from 74 to 78, indicating pseudo-tetraploidy (Figure 3). Despite the pseudo-tetraploidy observed in the AJ02-NM_0 cells by SKY analysis, CGH showed a relative loss of chromosomes 4 and 14 (Table 1).

A/J colon tumors display low-level MSI

Since the majority of AOM-induced colon tumors lacked CIN, we evaluated the possibility that an MSI phenotype may be associated with this model. Accordingly, we screened a panel of 11 loci comprising two mono- and nine dinucleotide repeats for MSI. Furthermore, an additional set of two short mononucleotide repeats, *JH102* and *JH104*, was analysed for insertion/deletion mutations by direct DNA sequencing. Each sample analysed for MSI at a given locus were replicated three times and each replicate experiment was performed using a new PCR reaction. Visual observation of the peak patterns showed striking consistency between the three replicates for each sample. The tumors were then classified into distinct MSI categories based on the National Cancer Institute criteria described above. An MSI-L phenotype was evident in 13/16 tumors, of which 77% were unstable at two loci and 23% at one locus (Table 1). Notably, all of the instabilities were restricted to dinucleotide repeats, an observation that is in agreement with earlier reports showing that alterations in mononucleotide runs are not characteristic of MSI-L cancers (Jass *et al*., 2002). In all, 3/16 tumors were stable at each of the loci examined and were therefore categorized as MSS. The AJ02-NM_0 cell line, however, revealed an MSI-H phenotype with instability at nine loci (Table 1). All of the MSI-L tumors, in addition to

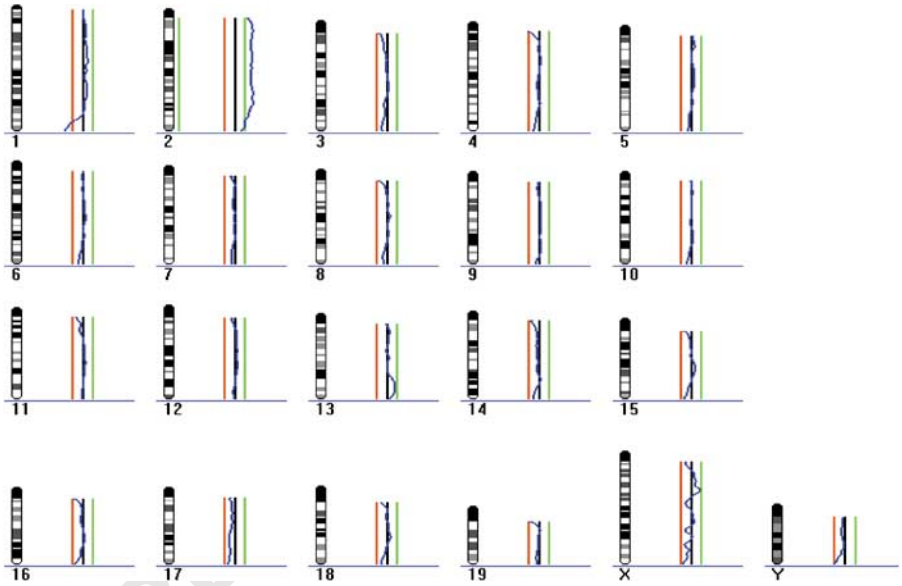

Figure 2 CGH profile of tumor E1. An average CGH summary profile of tumor E1, one of the two tumors displaying a gain of chromosome 2, is shown in the figure. The numbers at the bottom of the ideograms represent chromosome numbers. Solid bars to the right of the ideograms represent the threshold for gain (green) or loss (red) of chromosomal regions. The tortuous blue line in the center of the solid bars indicates the average ratio profile (tumor/control) along the entire length of each chromosome. The gain of chromosome 2 is the only copy number alteration observed in this tumor

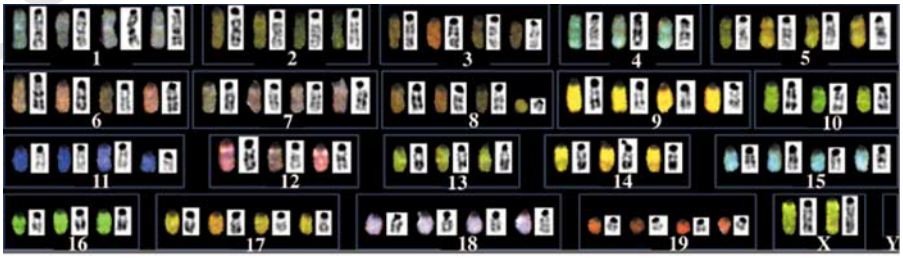

Figure 3 Chromosomal aberrations in AJ02-NM_0 tumor-derived cell line. Representative karyotype from SKY analysis displaying the spectral and corresponding inverted DAPI images for each chromosome. The numbers at the bottom of the individual boxes represent the chromosome number. A pseudo-tetraploidy condition, as described in Results and Discussion sections, together with the absence of chromosomal rearrangements, was evident in these cells. A loss of Y chromosome was detected by SKY analysis in these cells

UNCORRECTED

the AJ02-NM_0 cells, were unstable at the *D15Mit93* locus (Figure 4). Furthermore, none of the samples showed insertion/deletion mutations within the short mononucleotide repeats *JH102* and *JH104*.

Altered expression of β*-catenin in A/J colon tumors*

The role of K-ras, Apc, and *β*-catenin in the multistage progression of human colon cancers is firmly established (Calvert and Frucht, 2002; Kolligs *et al*., 2002). In the present study, we examined the mutational status of the K-*ras* and *Apc* genes in AOM-induced tumors. With the exception of one tumor, which showed a G***G***T→G***A***T transition mutation in codon 12, none of the samples, including the AJ02-NM_0 cells, revealed mutations within exon 1 of the K-*ras* oncogene (Vogelstein *et al*., 1988; Kislitsin *et al*., 2002; Brink *et al*., 2003; Corpet and Pierre, 2003). Furthermore, no sequence alterations were identified within the mutational cluster region (MCR) of the *Apc* gene (Fearnhead *et al*., 2001). Immunohistochemical analysis of Apc using an antibody directed against the C-terminus showed no loss of protein expression in representative tumor sections, providing additional evidence for the absence of truncation mutations within the Apc gene (Figure 5a–d). Furthermore, the nuclear staining pattern of Apc (Figure 5a–d) is consistent with earlier studies demonstrating significant nuclear localization of this protein within colonic epithelial cells (Wong *et al*., 1996; Neufeld and White, 1997). Despite the apparent lack of defects in the Apc protein, immunohistochemical analyses of *β*-catenin showed an intense nuclear accumulation in serially sectioned tumor epithelial cells (Figure 5e–h). On average, ~60% of the cells within each tumor crypt showed strong nuclear staining for *β*-catenin. In the AOM-treated mice, tumor cells stained more intensely for *β*-catenin than adjacent normal tissue (Figure 5f and g). More importantly, while a bilateral membrane-staining pattern for *β*-catenin was evident in the adjacent non-neoplastic crypts, an intense nuclear accumulation with minimal membrane staining was observed within the tumor cells (Figure 5g). Furthermore, no apparent changes in the staining intensity between the crypt epithelia and the surface columnar epithelial cells were observed in the non-neoplastic tissue (data not shown). Since *β*-catenin is the key downstream target of the Wnt signaling pathway, these data indicate that a pronounced disruption in this important proliferative pathway has occurred in A/J tumors.

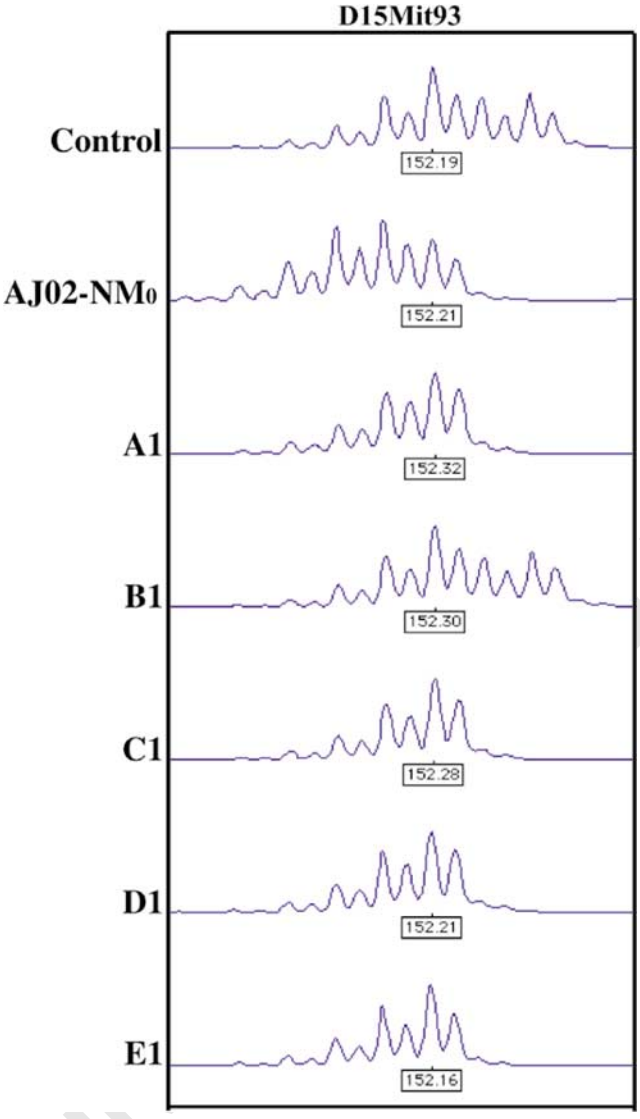

Figure 4 MSI at the *D15Mit93* locus in AOM-induced A/J tumors and AJ02-NM_0 cells. Representative microsatellite patterns from vehicle control, AJ02-NM_0 cells and A/J tumors, analysed using Genescan and Genotyper software (Applied Biosystems), are shown above. A1–E1 represent tumors from five different AOM-treated A/J mice. The patterns from the control animals were used as a reference to determine instability at a given locus. The numbers underneath the peaks in each sample specify the fragment size in bp. Note the shift in size and number of peaks in AJ02-NM_0 cells and the missing fragments in the tumors, A1, C1, D1, and E1, when compared to the control. The tumor, B1, showed a similar pattern to the control, and was classified as MSS for the locus

Discussion

CIN and aneuploidy are predominant features of human CRCs and many other solid tumors (Ried *et al*., 1999; Rajagopalan *et al*., 2003). In fact, CIN is by far the major form of genomic instability observed in the multi-step progression model of human CRCs (Ried *et al*., 1996; Hermsen *et al*., 2002; Hoglund *et al*., 2002; Goel *et al*., 2003). In the present study, using CGH and SKY techniques, we show that the acquisition of recurrent chromosomal aneuploidies is a less common feature of both primary tumors and cultured cells from carcinogen-treated mice (Table 1, Figure 3). It should be noted, however, that there was one recurring aberration, a gain of chromosome 2 that was observed in 12.5% of the primary colon tumors (Table 1). Interestingly, mouse chromosome 2 is partly orthologous to the q arm of human chromosome 20 that also shows a frequent gain in human CRCs (Human-Mouse Homology Map, http://www.ncbi.nlm.nih.gov/Homology/).

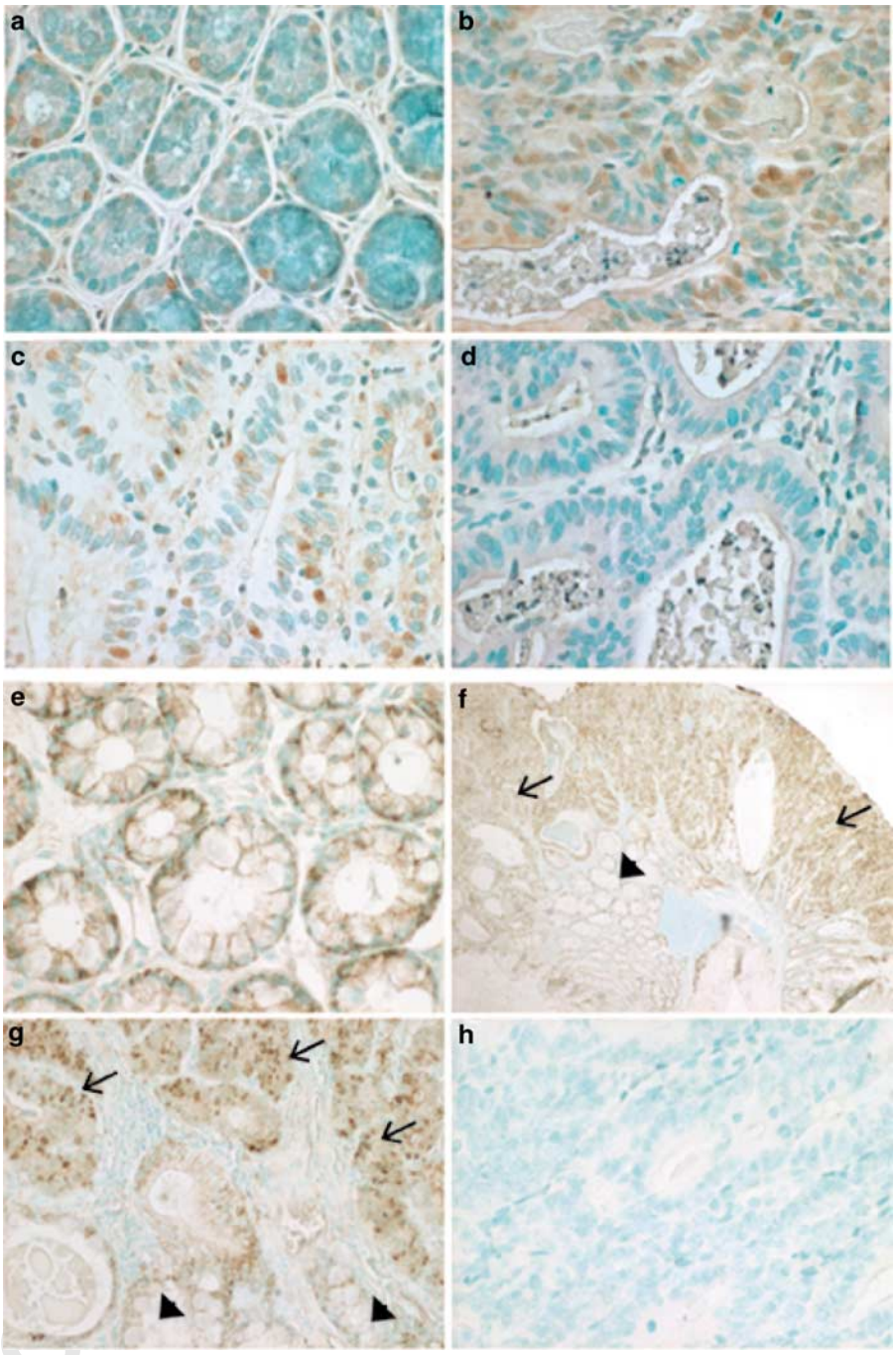

Figure 5 Immunohistochemical analysis of Apc and β-catenin in control colons and A/J tumors. Immunostaining for Apc in representative tissue sections (magnification $\times 400$) from a vehicle control colon (**a**), A/J colon tumors (**b**, **c**), and a negative control (**d**), in which rabbit IgG was used in place of the Apc-specific primary antibody. Apc immunoreactivity (brown staining) was localized primarily to the nucleus of the colonic epithelial cells in both control and tumor sections. Immunostaining for β-catenin in representative tissue sections from a vehicle control colon (**e**) $\times 400$, and A/J colon tumor (**f**) $\times 40$. Panel g is a higher magnification ($\times 200$) image of (**f**), and (**d**) represents the negative control, in which mouse IgG was used in place of β-catenin-specific primary antibody, $\times 200$. Open arrows indicate the tumor tissue and arrowheads indicate the adjacent normal-appearing crypts. A bilateral membrane-staining pattern of β-catenin (brown staining) was evident in the control colons as well as in the normal-appearing crypts adjacent to the tumor cells in AOM-treated mice. Note the predominantly nuclear localization of β-catenin in the tumor tissue. All the sections were counterstained with 0.5% methyl green

On the other hand, the pathogenetic significance of the loss of the Y chromosome in AOM-induced tumors, an event that occurs in human CRCs as well, remains unclear (Table 1, Figure 3). Despite the lack of gross chromosomal imbalances in the majority of primary tumors in the present study, there remains the possibility that aberrations within small chromosomal regions (<10 Mb) may be missed owing to the inherent

limitation of the CGH technique. Nevertheless, consistent with our findings, an earlier study in rats using genome-wide allelotyping showed that allelic imbalances are rare in AOM-induced (Wistar Furth × Fischer 344) F1 rat colon tumors (Haag *et al*., 1999). In contrast, Luceri *et al*. (2000), using a random amplified polymorphic DNA method, showed evidence of genomic instability in colon tumors from AOM-treated male Fischer 344 rats. The discrepancy between these earlier studies may be a result of the different rat strains used or the methodology employed for measuring CIN.

An alternative mechanism of genomic instability, the 'mutator' or the MSI pathway, results from a defective DNA mismatch repair system and is characterized by high-level instability in repeated nucleotide sequences. Such alterations may confer a selective growth advantage to cells during tumorigenesis, potentially resulting in frameshift mutations within several key tumor-suppressor genes that encode nucleotide repeats (Jass *et al*., 2002). The National Cancer Institute has developed criteria to classify MSI into three categories based on a panel of microsatellite repeat markers as MSI-H, MSI-L, and MSS (Jass *et al*., 2002). While most human CRCs typically show no evidence of MSI, approximately 10% of all sporadic and almost all HNPCC tumors display the 'mutator' phenotype (Young *et al*., 2001). On the other hand, there is an emerging body of evidence to suggest that a MSI-L or 'mild mutator' phenotype may actually comprise a distinct tumorigenic pathway that may account for nearly 10% of sporadic cases of CRC (Iino *et al*., 1999; Jass *et al*., 1999, 2002; Kambara *et al*., 2001; Whitehall *et al*., 2001; Jass, 2003). However, the molecular and morphological criteria for distinguishing MSI-L from MSS remains controversial (Tomlinson *et al*., 2002; Jass, 2003). Based on the significance of the MSI phenotypes and given the fact that CIN and MSI are, in general, mutually exclusive events in human CRCs (Lothe *et al*., 1993; Thibodeau *et al*., 1993; Olschwang *et al*., 1997; Eshleman *et al*., 1998), we hypothesized that an MSI mechanism may be fundamental to the development of these chromosomally stable A/J tumors. Results showed a MSI-L in the majority of A/J tumors (Table 1, Figure 4), thereby suggesting the possibility for the presence of a 'mild mutator' mechanism active during carcinogen-induced tumorigenesis. If this is the case, then the expansion of MSI-L to MSI-H in the rapidly dividing AJ02-NM_0 cells (Table 1) may provide an experimental system for evaluating this possibility. It should be noted, however, that MSI, even at a low level, has seldom been observed in AOM-induced rat colon tumors (Haag *et al*., 1999; Walchle *et al*., 1999; Luceri *et al*., 2000), suggesting species-specific differences in the molecular mechanisms underlying chemical carcinogenesis.

The limited extent of chromosomal imbalance and only MSI-L observed in the A/J primary tumors suggested the likelihood that defects present in other critical pathways, in particular Apc/β-catenin, may play an important role in carcinogen-induced tumorigenesis. Surprisingly, there were no sequence alterations identified within the MCR of the *Apc* gene (Fearnhead *et al*., 2001). Further immunohistochemical analysis of Apc using an antibody directed against the C-terminus showed no loss of protein expression within representative tumor sections, providing additional evidence for the absence of truncation mutations within the *Apc* gene (Figure 5a–d). Furthermore, the nuclear staining pattern of Apc (Figure 5a–d) is consistent with earlier studies demonstrating significant nuclear localization of this protein in the epithelial cells (Wong *et al*., 1996; Neufeld and White, 1997). Nevertheless, our findings of intense nuclear accumulation of β-catenin (Figure 5e–h) in the absence of *Apc* truncation mutations indicate a dysregulated Wnt signaling pathway in AOM-induced colon tumors and such an observation was supported by several previous studies in murine models (De Filippo *et al*., 1998; Sheng *et al*., 1998; Takahashi *et al*., 2000a, b; Corpet and Pierre, 2003). However, one must not rule out the possibility that sequence alterations of the *Apc* gene may have occurred outside of the critical MCR that may adversely impact Wnt signaling.

In summary, we have investigated the role of genomic instability in a widely used colon carcinogen model. Our findings suggest that carcinogen-induced colon tumors may evolve via mechanisms that are independent of the classical 'suppressor' or 'mutator' pathway. These observations, however, do not rule out the significance of this animal model for studying colorectal tumorigenesis. In fact, several recent studies in human CRCs have also shown that a subset of human cancers do not fall within either of these two genetic pathways, regardless of tumor stage/grade (Georgiades *et al*., 1999; Chan *et al*., 2001; Goel *et al*., 2003), suggesting that the molecular mechanisms leading to colorectal tumorigenesis are not necessarily defined by either the CIN or MSI pathways alone.

Materials and methods

Animals and treatment

Male A/J mice, 5-week old, were purchased from the Jackson Laboratories (Bar Harbor, ME, USA) and housed in a temperature-controlled environment ($23 \pm 1^{\circ}$C) with a 12 h light/dark cycle. The mice were provided with Purina laboratory rodent chow and water *ad libitum*. After an acclimation period of 1 week, five mice were treated with AOM dissolved in 0.9% NaCl by intraperitoneal injections at a dose of 10 mg/kg body weight once a week for 6 weeks. An additional group of five mice received 0.9% NaCl alone and served as vehicle controls. Animals were killed 32 weeks after the last injection and tumors were harvested and evaluated by histomorphology. In all, 16 *in situ* adenocarcinomas (>4 mm) were used for all subsequent analyses. A total of 15 normal distal colon sections were harvested from the vehicle control mice. Genomic DNA was extracted using QIAamp DNA Mini kit (Qiagen, Valencia, CA, USA) as per the manufacturer's instructions and used for subsequent CGH, MSI, and mutational analyses.

NOT CORRECTED PROOF

Cell culture

Murine tumor cells referred to as AJ02-NM_0 were derived from an A/J colon tumor. Briefly, excised primary colon tumors were minced and serially transferred into immunodeficient nude (Nu/Nu) mice (Charles River Laboratories, Wilmington, MA, USA). Following two *subcutaneous* serial passages, the tumor cells were excised, minced, and a portion seeded onto a p60 dish. After 24 h, the dish was rinsed and irradiated feeder layers (fibroblast-like cells isolated from previous attempts at growing AOM-induced colon tumors from the same mouse strain) were added. After a month in culture, two dense colonies were subcloned using glass-cloning rings to yield a rapidly growing population of cells determined to be free from cells displaying fibroblast-like morphology. The AJ02-NM_0 cells grew in the absence of feeder layers and were passed into larger flasks. A flask designated passage 1 was seeded approximately 45 days after subcloning. Chromosome spreads for SKY analysis were prepared on AJ02-NM_0 cells at passage 12. In parallel, genomic DNA was extracted from these cells using the QIAamp DNA Mini kit (Qiagen) and was used to perform CGH, MSI, and mutational analyses. RPMI supplemented with 10% fetal bovine serum (Invitrogen, Carlsbad, CA, USA) served as the growth media for these cells.

Comparative genomic hybridization

DNA labeling, hybridization, and detection were performed as previously described (Weaver *et al*., 2002). Briefly, 2 μg of DNA from primary tumors or AJ02-NM_0 cells and saline control colons were labeled with biotin-16-dUTP and digoxigenin-11dUTP (Boehringer Mannheim, Indianapolis, IN, USA), respectively, by nick translation, and were ethanol precipitated in the presence of 10 μg of salmon sperm DNA and 40 μg of the Cot-I fraction of mouse DNA (Gibco BRL, Gaithersburg, MD, USA). This labeled DNA probe was resuspended in 10 μl of hybridization solution (50% formamide, 2 $\times$ sodium chloride and sodium citrate buffer (SSC), 10% dextran sulfate), denatured for 5 min at 80°C, and preannealed at 37°C for 1.5 h. Normal metaphase chromosomes from splenic cultures of C57BL/6 mice were dropped onto glass slides and pretreated with 0.1 mg/ml RNase (100 μg/ml), followed by 10 μg/ml pepsin in 0.01 M HCL. The chromosomes were denatured in 70% formamide, 2 $\times$ SSC at 80°C for 1.5 min prior to application of the probe DNA mixture. Hybridization was carried out at 37°C for 72 h in a humidifying chamber. Probe signals were detected using an amplification procedure and counterstained with 4′,6-diamidino-2-phenylindole (DAPI), as described previously (Weaver *et al*., 2002). Images were acquired with a cooled charge-coupled device (CCD) camera (Photometrics, Tuscon, AZ, USA) mounted on a Leica DMRXA epifluorescence microscope (Leica, Wetzlar, Germany) using filters specific for DAPI, fluorescein, and rhodamine (Chroma Technologies, Brattleboro, VT, USA). CGH ratio profiles were calculated using Leica Chantal software (Leica Imaging Systems, Cambridge, UK) as described earlier (Weaver *et al*., 2002).

Spectral karyotyping

Metaphase chromosomes for SKY hybridization were prepared from AJ02-NM_0 cells at passage 12. Cells in culture were incubated for 2 h in 0.02 μg/ml Colcemid (Invitrogen, Carlsbad, CA, USA). The cells were incubated in hypotonic solution (0.075 M KCl) and fixed in methanol : acetic acid (3 : 1). Spectral karyotyping was then performed as described previously, using a unique combination of five different fluorochromes (Liyanage *et al*., 1996; Weaver *et al*., 2002). Images were acquired with SkyView software (Applied Spectral Imaging, Ltd, Migdal Haemek, Israel) using a spectral cube and a CCD camera (Hamamatsu, Bridgewater, NJ, USA) connected to a DMRXA microscope (Leica) with a custom SKY-3 optical filter (Chroma Technology). At least 20 metaphases were imaged and karyotyped using SkyView software.

MSI analysis

Two mononucleotide (*uPAR*, *pro-1*) (Kohonen-Corish *et al*., 2002) and nine dinucleotide (*D1Mit62*, *D15Mit93*, *D17Mit72*, *D17Mit123*, *D17Mit185*, *D1Mit4*, *D7Mit17*, *D10Mit2*, and *D14Mit15*) repeat markers were utilized to determine MSI status in primary tumors and AJ02-NM_0 cells. Primer sequences for all dinucleotide markers were obtained from the Whitehead Institute for Biomedical Research/Massachusetts Institute of Technology, Centre for Genome Research database (http://www.genome.wi.mit.edu). One primer from each primer pair was synthesized with a 5′ fluorescent tag (FAM). PCR amplification was performed in a total volume of 50 μl, containing 50–100 ng of genomic DNA, 2.5 mM $MgCl_2$, 0.2 mM each dATP, dGTP, dCTP, and dTTP, 0.25 μM each forward and reverse primers, and 1.25 U of Taq DNA polymerase (Invitrogen). PCR reactions were carried out in a PTC-200, Peltier Thermal Cycler (MJ research Inc, Reno, NV, USA), which included an initial denaturation at 94°C for 2 min followed by 94°C (45 s), 57°C (30 s), and 72°C (30 s) for 35 cycles, and a final elongation at 72°C for 5 min. Fragments were visualized using an ABI 377 Sequencer (Applied Biosystems, Foster City, CA, USA). Data were analysed using Genescan and Genotyper software (Applied Biosystems). Colon tumors including AJ02-NM_0 cells were scored as having instability at a given locus if there was a significant shift in size, number of the peaks, and/or the pattern of microsatellite repeat regions when compared to the consistent pattern of peaks produced by the vehicle control colon samples. As an additional control experiment for AJ02-NM_0 cells, the microsatellite patterns from 11 markers were compared with those obtained from the tail DNA of immunodeficient nude (Nu/Nu) mice. To rule out artifacts inherent to the PCR process due to polymerase slippage, or to migration errors in the gel, instability at a marker locus was scored only when microsatellite alterations could be reproduced in repeat PCR reactions. Based on the National Cancer Institute criteria (Jass *et al*., 2002), samples were then classified as MSI-H when $>30\%$ of marker loci examined showed signs of instability, MSI-L (instability at $<30\%$ of marker loci) or MSS (no instability at any of the markers examined). In addition, two short mononucleotide repeats, *JH102* and *JH104*, which have been previously reported to be good indicators of instability in tumors of *Mlh1*-deficient mice (Kohonen-Corish *et al*., 2002), were analysed for insertion–deletion mutations by direct sequencing in AOM-induced tumors and AJ02-NM_0 cells.

*Screening for K-*ras *and* Apc *gene mutation*

The K-*ras* oncogene was analysed for AOM-induced sequence alterations in A/J tumors and AJ02-NM_0 cells. PCR amplification for K-*ras* exon 1, using forward 5′-TGTAAGGCCTGCTGAAAATG-3′ and reverse 5′-GCACGCAGACTGTAGAGCAG-3′ primers, was carried out at 95°C for 5 min followed by 95°C (30 s), 55°C (30 s), and 72°C (45 s) for 35 cycles, and a final elongation at 72°C for 5 min. The PCR products were then sequenced using ABI 377 sequencer (Applied Biosystems). Similarly, a 2.74 kb fragment in exon 15

UNCORRECTED PROOF

of the *Apc* gene, which includes the MCR, was PCR amplified and analysed for sequence alterations using three sets of overlapping primers as previously described (Sohn *et al*., 2003).

Apc and β*-catenin immunohistochemistry*

Formalin-fixed, paraffin-embedded mouse colon tumor and vehicle control tissue sections (5 μm) were subjected to antigen retrieval with 10 mM citrate buffer and incubated at 4°C overnight with rabbit polyclonal anti-APC (C-20), raised against a peptide mapping to the carboxy terminus of the human APC protein (Santa Cruz Biotechnology, Santa Cruz, CA, USA), at a dilution of 1 : 20 in PBS. Sections were washed with PBS/Brij and incubated with biotinylated goat anti-rabbit immunoglobulin G (Vector Laboratories, Burlingame, CA, USA) at a dilution of 1 : 200 at room temperature for 30 min. After washing, the sections were incubated with avidin–biotin peroxidase complex provided by Vectastain Elite ABC kit (Vector Laboratories) at room temperature for 30 min. Color was developed with 3,3-diaminobenzidine as the substrate and the sections were counterstained with 0.5% methyl green. As a negative control, duplicate sections were immunostained with rabbit IgG in place of the APC primary antibody. In addition, a similar analysis was performed on serial sections obtained from the same tissues, except that they were not subjected to the antigen-retrieval procedure before incubating with the primary antibody. Furthermore, the procedure was repeated with a second APC antibody obtained from a different batch (Santa Cruz Biotechnology). For β-catenin immunostaining, serial sections of A/J tumors and vehicle-treated control colons were incubated at 4°C overnight with mouse monoclonal anti-β-catenin antibody (Sigma-Aldrich, St Louis, MO, USA) at a dilution of 1 : 1000 in 10% normal goat serum. The sections were then washed and incubated with biotinylated goat anti-mouse immunoglobulin G at a dilution of 1 : 100 (Vector Laboratories, Burlingame, CA, USA) at room temperature for 30 min. After washing, the sections were incubated with avidin–biotin peroxidase complex at room temperature for 30 min using the Vectastain Elite ABC kit (Vector laboratories). Color was developed using 3,3′-diaminobenzidine substrate and sections were counterstained with 0.5% methyl green (Trevigen Inc., Gaithersburg, MD, USA). As a negative control, duplicate sections were immunostained with mouse IgG in place of the primary β-catenin antibody. Furthermore, Apc and β-catenin-positive cells were counted in a minimum of 10 different high magnification ($\times 400$) fields per section.

Abbreviations

AOM, azoxymethane; CRC, colorectal cancer; CGH, comparative genomic hybridization; CIN, chromosomal instability; MSI, microsatellite instability; MSS, microsatellite stable; MSI-L, low-level microsatellite instability; MSI-H, high-level microsatellite instability; SKY, spectral karyotyping; FAP, familial adenomatous polyposis; HNPCC, hereditary nonpolyposis colorectal cancer; K-ras, Kirsten rat sarcoma oncogene; Apc, adenomatosis polyposis coli; MCR, mutational cluster region; MMR, mismatch repair.

Acknowledgements

This work was supported in part by NIH grant CA81428 to DWR.

References

Brink M, de Goeij AF, Weijenberg MP, Roemen GM, Lentjes MH, Pachen MM, Smits KM, de Bruine AP, Goldbohm RA and van den Brandt PA. (2003). *Carcinogenesis*, **24,** 703–710.

Calvert PM and Frucht H. (2002). *Ann. Intern. Med.*, **137,** 603–612.

Chan TL, Curtis LC, Leung SY, Farrington SM, Ho JW, Chan AS, Lam PW, Tse CW, Dunlop MG, Wyllie AH and Yuen ST. (2001). *Oncogene*, **20,** 4871–4876.

Corpet DE and Pierre F. (2003). *Cancer Epidemiol. Biomarkers Prev.*, **12,** 391–400.

De Filippo C, Caderni G, Bazzicalupo M, Briani C, Giannini A, Fazi M and Dolara P. (1998). *Br. J. Cancer*, **77,** 2148–2151.

Dong M, Guda K, Nambiar PR, Rezaie A, Belinsky GS, Lambeau G, Giardina C and Rosenberg DW. (2003). *Carcinogenesis*, **24,** 307–315.

Eshleman JR, Casey G, Kochera ME, Sedwick WD, Swinler SE, Veigl ML, Willson JK, Schwartz S and Markowitz SD. (1998). *Oncogene*, **17,** 719–725.

Fearnhead NS, Britton MP and Bodmer WF. (2001). *Hum. Mol. Genet.*, **10,** 721–733.

Fearon ER and Vogelstein B. (1990). *Cell*, **61,** 759–767.

Georgiades IB, Curtis LJ, Morris RM, Bird CC and Wyllie AH. (1999). *Oncogene*, **18,** 7933–7940.

Goel A, Arnold CN, Niedzwiecki D, Chang DK, Ricciardiello L, Carethers JM, Dowell JM, Wasserman L, Compton C, Mayer RJ, Bertagnolli MM and Boland CR. (2003). *Cancer Res.*, **63,** 1608–1614.

Guda K, Giardina C, Nambiar P, Cui H and Rosenberg DW. (2001). *Mol. Carcinog.*, **31,** 204–213.

Haag JD, Brasic GM, Shepel LA, Newton MA, Grubbs CJ, Lubet RA, Kelloff GJ and Gould MN. (1999). *Mol. Carcinog.*, **24,** 47–56.

Hermsen M, Postma C, Baak J, Weiss M, Rapallo A, Sciutto A, Roemen G, Arends JW, Williams R, Giaretti W, De Goeij A and Meijer G. (2002). *Gastroenterology*, **123,** 1109–1119.

Hoglund M, Gisselsson D, Hansen GB, Sall T, Mitelman F and Nilbert M. (2002). *Cancer Res.*, **62,** 5939–5946.

Iino H, Jass JR, Simms LA, Young J, Leggett B, Ajioka Y and Watanabe H. (1999). *J. Clin. Pathol.*, **52,** 5–9.

Jass JR. (2003). *J. Pathol.*, **199,** 267–269 author reply 269–70..

Jass JR, Biden KG, Cummings MC, Simms LA, Walsh M, Schoch E, Meltzer SJ, Wright C, Searle J, Young J and Leggett BA. (1999). *J. Clin. Pathol.*, **52,** 455–460.

Jass JR, Walsh MD, Barker M, Simms LA, Young J and Leggett BA. (2002). *Eur. J. Cancer*, **38,** 858–866.

Kambara T, Matsubara N, Nakagawa H, Notohara K, Nagasaka T, Yoshino T, Isozaki H, Sharp GB, Shimizu K, Jass J and Tanaka N. (2001). *Cancer Res.*, **61,** 7743–7746.

Kislitsin D, Lerner A, Rennert G and Lev Z. (2002). *Dig. Dis. Sci.*, **47,** 1073–1079.

Kohonen-Corish MR, Daniel JJ, te Riele H, Buffinton GD and Dahlstrom JE. (2002). *Cancer Res.*, **62,** 2092–2097.

Kolligs FT, Bommer G and Goke B. (2002). *Digestion*, **66,** 131–144.

Lengauer C, Kinzler KW and Vogelstein B. (1997). *Nature*, **386,** 623–627.

Lindblom A. (2001). *Curr. Opin. Oncol.*, **13,** 63–69.

Liyanage M, Coleman A, du Manoir S, Veldman T, McCormack S, Dickson RB, Barlow C, Wynshaw-Boris A,

UNCORRECTED PROOF

Janz S, Wienberg J, Ferguson-Smith MA, Schrock E and Ried T. (1996). *Nat. Genet.*, **14,** 312–315.

Lothe RA, Peltomaki P, Meling GI, Aaltonen LA, Nystrom-Lahti M, Pylkkanen L, Heimdal K, Andersen TI, Moller P and Rognum TO *et al*. (1993). *Cancer Res.*, **53,** 5849–5852.

Luceri C, De Filippo C, Caderni G, Gambacciani L, Salvadori M, Giannini A and Dolara P. (2000). *Carcinogenesis*, **21,** 1753–1756.

Nambiar PR, Giardina C, Guda K, Aizu W, Raja R and Rosenberg DW. (2002). *Cancer Res.*, **62,** 3667–3674.

Nambiar PR, Girnun G, Lillo NA, Guda K, Whiteley HE and Rosenberg DW. (2003). *Int. J. Oncol.*, **22,** 145–150.

Neufeld KL and White RL. (1997). *Proc. Natl. Acad. Sci. USA*, **94,** 3034–3039.

Olschwang S, Hamelin R, Laurent-Puig P, Thuille B, De Rycke Y, Li YJ, Muzeau F, Girodet J, Salmon RJ and Thomas G. (1997). *Proc. Natl. Acad. Sci. USA*, **94,** 12122–12127.

Rajagopalan H, Nowak MA, Vogelstein B and Lengauer C. (2003). *Nat. Rev. Cancer*, **3,** 695–701.

Ried T, Heselmeyer-Haddad K, Blegen H, Schrock E and Auer G. (1999). *Genes Chromosomes Cancer*, **25,** 195–204.

Ried T, Knutzen R, Steinbeck R, Blegen H, Schrock E, Heselmeyer K, du Manoir S and Auer G. (1996). *Genes Chromosomes Cancer*, **15,** 234–245.

Sheng H, Shao J, Williams CS, Pereira MA, Taketo MM, Oshima M, Reynolds AB, Washington MK, DuBois RN and Beauchamp RD. (1998). *Carcinogenesis*, **19,** 543–549.

Sohn KJ, Choi M, Song J, Chan S, Medline A, Gallinger S and Kim YI. (2003). *Carcinogenesis*, **24,** 217–224.

Takahashi M, Mutoh M, Kawamori T, Sugimura T and Wakabayashi K. (2000a). *Carcinogenesis*, **21,** 1319–1327.

Takahashi M, Nakatsugi S, Sugimura T and Wakabayashi K. (2000b). *Carcinogenesis*, **21,** 1117–1120.

Thibodeau SN, Bren G and Schaid D. (1993). *Science*, **260,** 816–819.

Tomlinson I, Halford S, Aaltonen L, Hawkins N and Ward R. (2002). *J. Pathol.*, **197,** 6–13.

Vogelstein B, Fearon ER, Hamilton SR, Kern SE, Preisinger AC, Leppert M, Nakamura Y, White R, Smits AM and Bos JL. (1988). *N. Engl. J. Med.*, **319,** 525–532.

Walchle C, Diwan BA, Shiao YH and Calvert RJ. (1999). *Toxicol. Appl. Pharmacol.*, **157,** 9–15.

Wang QS, Papanikolaou A, Sabourin CL and Rosenberg DW. (1998). *Carcinogenesis*, **19,** 2001–2006.

Weaver Z, Montagna C, Xu X, Howard T, Gadina M, Brodie SG, Deng CX and Ried T. (2002). *Oncogene*, **21,** 5097–5107.

Whitehall VL, Walsh MD, Young J, Leggett BA and Jass JR. (2001). *Cancer Res.*, **61,** 827–830.

Wong MH, Hermiston ML, Syder AJ and Gordon JI. (1996). *Proc. Natl. Acad. Sci. USA*, **93,** 9588–9593.

Young J, Simms LA, Biden KG, Wynter C, Whitehall V, Karamatic R, George J, Goldblatt J, Walpole I, Robin SA, Borten MM, Stitz R, Searle J, McKeone D, Fraser L, Purdie DR, Podger K, Price R, Buttenshaw R, Walsh MD, Barker M, Leggett BA and Jass JR. (2001). *Am. J. Pathol.*, **159,** 2107–2116.

UNCORRECTED PROOF